



Fragility Functions of SDOF Systems by Accelerograms with Spectra Variable in Shape with Magnitude

Francesca Barbagallo¹, Melina Bosco², Aurelio Ghersi³, Edoardo M. Marino⁴, Pier Paolo Rossi⁴

¹ Assistant Researcher, ² Assistant Professor, ³ Full Professor,

⁴ Associate Professor, Department of Civil Engineering and Architecture, University of Catania, Italy.

ABSTRACT

Numerous researchers have proposed methodologies for the evaluation of the fragility function of a building, e.g. by means of incremental dynamic analysis or multiple stripe analysis. However, in almost every case, numerical analyses are carried out by means of a single set of accelerograms that is scaled in acceleration to simulate earthquakes with different magnitude. Therefore, these numerical analyses neglect that other seismological parameters (e.g. the shape of the pseudo-acceleration response spectrum and the significant duration of the accelerogram) may vary with the magnitude of the earthquake. This simplification in the seismic assessment of buildings is generally due to the difficulty in selecting or generating accelerograms that are compatible with multiple seismological parameters. In this paper, the multiple stripe analysis is applied to SDOF systems with different inelastic responses taking into account also the variation in the shape of the pseudo-acceleration response spectrum as a function of magnitude, as suggested by the National Institute of Geophysics and Volcanology for the Italian territory. To this end, several sets of artificial accelerograms are generated by means of the program SIMKQE so that each set is compatible with a pseudo-acceleration response spectrum characterized by an assigned magnitude. The results highlight the importance of the shape of the response spectrum on the fragility function of SDOF systems and relate it to the period of vibration of the system and the degradation of the response of the system.

Keywords: Fragility function, mean annual frequency of exceedance, multi-stripe analysis, artificial accelerograms.

INTRODUCTION

To obtain the probabilistic seismic assessment of buildings, the response is commonly obtained by means of Incremental Dynamic Analysis (IDA) or Multiple-Stripe Analysis (MSA) [[1]. In nearly all cases, the numerical analyses are carried out with a single suite of accelerograms, which is compatible - from the probabilistic point of view - with a specified elastic response spectrum and scaled in intensity to simulate earthquakes of different magnitude. This simplification is compatible with the description of the ground motion characteristics and effects reported in most seismic codes, but it is not in line with the most recent advances in the field and with the state-of-art knowledge. The use of scaled ground motions is strongly encouraged if natural accelerograms are considered, owing to the difficulty in selecting suites of natural ground motions that are compatible with different and multiple seismological parameters. A similar approach is followed also if artificial accelerograms are generated, most likely because of the greater computational burden deriving from the generation of multiple suites of accelerograms. However, the results of the probabilistic assessment of the seismic response of structures appear to be questionable in accuracy because of the influence of the shape of the elastic response spectrum on the inelastic response of structures. Moreover, the authors note that the Italian seismic code [[2] already prescribes the evaluation of both the shape and intensity of the elastic pseudo-acceleration spectrum as a function of the earthquake return period and that recent papers have put the basis for a similar modification of Eurocode 8 [[3].

The impact of the above limitations on the assessment of the seismic performance of buildings is investigated in this paper. In particular, the fragility function and the mean annual frequency of exceedance of assigned limit states are calculated by multiple stripe analysis by means of artificial accelerograms that reflect or neglect (i) the variation in shape of the elastic response spectrum and (ii) the variation of the ground motion duration with the selected Intensity Measure (IM). The single MSA considers different suites of artificial accelerograms, each one being generated to be compatible with an assumed elastic response spectrum and ground motion duration. The compatibility is achieved in terms of the median value and standard deviation for the elastic spectral response and only in terms of the median value for the ground motion duration. The data provided by the National Institute of Geophysics and Volcanology (INGV) for the Italian territory [[4] are used to define the elastic response spectra corresponding to increasing IM levels. The equations proposed by Bommer et al. [[5] are used to estimate the ground motion duration based on the seismic hazard disaggregation results provided by the INGV. The suites of

targeted elastic response spectra are generated by means of the method proposed by Zentner [[6], whereas the artificial accelerograms are obtained using the program SIMQKE. An additional MSA analysis is performed to evaluate the effects of the dispersion of the elastic spectral accelerations on the structural response. To this end, the suites of accelerograms are generated so that their elastic response spectra have an equal shape and thus an almost null standard deviation about the mean value. The fragility function and the mean annual frequency of exceedance are calculated here on a large set of single-degree-of-freedom (SDOF) systems characterised by different degrading or non-degrading inelastic responses.

FRAGILITY FUNCTION AND MEAN ANNUAL FREQUENCY OF EXCEEDANCE OF LIMIT STATES

The fragility function is determined by multiple-stripe analysis, so that different suites of accelerograms can be considered as corresponding to different earthquake return periods. To make the number of ground motions adequate for a probabilistic seismic analysis, 30 ground motions are considered for each earthquake return period. The suites of ground motions are artificially generated to be compatible with elastic response spectra varying in shape and intensity with the earthquake return period, in keeping with the data reported by the INGV for the Italian territory (www.ingv.it). The intensity measure of each suite of ground motions is the median spectral acceleration at the fundamental period of vibration of the system.

The maximum likelihood method is applied to obtain the fragility functions. At each intensity level $IM = x_j$, the structural analyses produce a certain number of cases that exceed the given limit state out of the total number of ground motions. The probability of observing z_j cases of exceedance out of n_j ground motions with $IM = x_j$ is given by the binomial distribution

$$P(z_j \text{ exceedances in } n_j \text{ ground motions}) = \binom{n_j}{z_j} p_j^{z_j} (1 - p_j)^{n_j - z_j} \quad (1)$$

where p_j is the probability that a ground motion with $IM = x_j$ will cause exceedance of the specified limit state function. When analysis data is obtained at multiple IM levels, the product of the above binomial probabilities at each IM level gives the likelihood for the entire data set, i.e.

$$\text{Likelihood} = \prod_{j=1}^m \binom{n_j}{z_j} p_j^{z_j} (1 - p_j)^{n_j - z_j} \quad (2)$$

where m is the number of IM levels and Π is a product over all levels. A lognormal cumulative distribution function is used to define the fragility function

$$P(C|IM=x) = \Phi \left[\frac{\ln(x/\theta)}{\beta} \right] \quad (3)$$

where $P(C|IM=x)$ is the probability of exceedance of a limit state function due to a ground motion with $IM=x$, $\Phi()$ is the standard normal cumulative distribution function (CDF), θ is the median of the fragility function (the IM level with 50% probability of exceedance) and β is the standard deviation of $\ln IM$. The fragility function parameters are obtained by maximizing the logarithm of the likelihood function, as reported in the following relationship [[7]

$$\{\hat{\theta}, \hat{\beta}\} = \arg \max_{\theta, \beta} \sum_{j=1}^m \left\{ \ln \binom{n_j}{z_j} + z_j \ln \Phi \left(\frac{\ln(x_j/\theta)}{\beta} \right) + (n_j - z_j) \ln \left[1 - \Phi \left(\frac{\ln(x_j/\theta)}{\beta} \right) \right] \right\} \quad (4)$$

SEISMIC HAZARD

The probabilistic seismic hazard analysis results from project S1 developed by the INGV and the Department of Civil Protection of Italy. This project defined the probabilistic seismic hazard at the points of a regular grid (step equal to 0.05° in latitude and longitude) over the entire Italian territory. Some results are reported in tables in the current Italian code NTC2008 regarding the parameters characterising the elastic response spectra corresponding to a viscous damping ratio equal to 0.05 [[2]. The elastic response spectra are specified for three different fractiles of the maximum spectral accelerations (equal to 16, 50 and 84%) and for nine different probabilities of exceedance P_{VR} (2, 5, 10, 22, 30, 39, 50, 63 and 81%) in a reference period of time of 50 years. The return periods T_R corresponding to the above probabilities of exceedance P_{VR} and reference period of time are equal to 2500, 1000, 475, 200, 140, 100, 72, 50 and years. The spectral accelerations are reported for ten periods of vibration (equal to 0.10, 0.15, 0.20, 0.30, 0.40, 0.50, 0.75, 1.00, 1.50 and 2.00 s) and refer to rigid soil (average shear-wave velocity V_{s30} over the uppermost 30 m at the site greater than 800 m/s). In addition, a dedicated web site (www.ingv.it) allows users to visualize the elastic response spectra corresponding to a specified point of the Italian territory and to know the results of a disaggregation analysis for the peak ground acceleration.

The site considered in this paper for numerical analyses is near Siracusa (Sicily), in the south of Italy, and is identified by ID

number 49418 in the website. The seismic hazard of this site is significantly governed by a single seismogenic source. The suites of artificially generated ground motions are compatible with the seismic hazard of this site in terms of median spectral acceleration, standard deviation of the spectral accelerations at given periods of vibration and in terms of correlation coefficients between spectral accelerations at different periods of vibration. The ground motions are also compatible with the mean values of the expected significant duration as defined by Bommer et al. [[5]. Assuming that the distribution of the spectral accelerations is lognormal, the logarithmic standard deviation $\sigma_{\ln S_a}$ of the spectral accelerations corresponding to the specified site and to a given period of vibration and probability of exceedance is calculated by means of the following relationship

$$\sigma_{\ln S_a} = 0.5 \left(\ln S_{a,84\%} - \ln S_{a,16\%} \right) \quad (5)$$

where $S_{a,84\%}$ and $S_{a,16\%}$ are the spectral accelerations corresponding to the 84% and 16% fractiles. The mean values of the spectral accelerations are obtained from the 50% fractile and variance of the spectral accelerations as

$$S_{\text{mean}} = \exp \left(\ln S_{a,50\%} + \sigma_{\ln S_a}^2 / 2 \right) \quad (6)$$

For periods of vibration lower than 2.00 s the spectral acceleration is assumed to vary linearly between the values reported by INGV. Instead, for periods of vibration higher than 2.00 s the spectral accelerations are calculated assuming that the spectral displacement remains constant and equal to the value corresponding to a period of 2 s. To achieve a more accurate evaluation of the fragility function for earthquake return periods around 475 years, other two pseudo-acceleration spectra have been constructed. They correspond to probabilities of exceedance equal to 7% and 16% in 50 years, i.e. return periods equal to 689 and 287 years, according to CNR-DT 212/2013 [[8]. To accomplish this task, the seismic hazard curves have been determined in terms of spectral acceleration for each considered period of vibration and fractile of the spectral accelerations. As suggested in CNR-DT 212/2013 [[8], the hazard curve is calculated as

$$\lambda_s(S_a) = \frac{1}{T_R} \quad \text{for} \quad S_a = S_{a,16\%}, S_{a,50\%} \text{ or } S_{a,84\%} \quad (7)$$

A quadratic function has been calibrated in a logarithmic space to match the relation between the mean hazard curve and the spectral acceleration S at each period of vibration of interest, i.e.

$$\lambda_s(S_a) = k_0 \exp \left(-k_1 \ln S_a - k_2 \ln^2 S_a \right) \quad (8)$$

Parameters k_0 , k_1 and k_2 have been determined by means of an iterative procedure so as to minimize the distance between the points provided by INGV and the points of the analytical curve. Once their value is determined, the spectral acceleration corresponding to prefixed values of return periods can be determined. The median acceleration spectra are plotted in Figure 1a for all the return periods considered in this study.

Generation of artificial accelerograms

The target elastic response spectra and the corresponding accelerograms have been generated by means of the method suggested by Zentner [[6]. Each suite of ground motions is composed of 30 accelerograms. The target elastic response spectra of each suite are defined to have the same median and standard deviation as the elastic response spectra defined by the INGV for the considered site and return period. To consider correlations of spectral accelerations at different periods, the correlation equations developed by Cimellaro [[9] for European sites are applied. To this end, the residual is first normalised to the standard deviation as

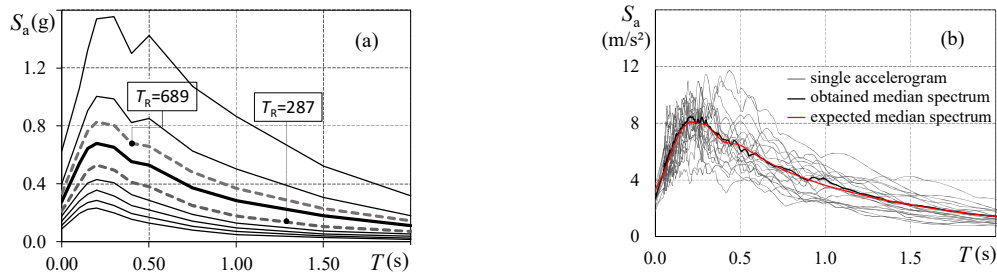


Figure 1. (a) Median pseudo-acceleration spectra and (b) pseudo-acceleration spectra of the single accelerograms and obtained and expected median pseudo-acceleration spectra of the suites of accelerograms ($T_R=689$).

$$\varepsilon(T) = \left[\log_{10} S_a(T) - \mu_{\log_{10} S_a(T)} \right] / \sigma_{\log_{10} S_a(T)} \quad (9)$$

where $\log_{10} S_a(T)$ is the logarithm in base 10 (as considered by Cimellaro [[9]]) of the observed spectral acceleration, $\mu_{\log_{10} S_a(T)}$ and $\sigma_{\log_{10} S_a(T)}$ are the mean and standard deviation of the logarithm of the spectral accelerations, respectively. Then, the values reported in [[9]] are forced to the correlation coefficients $\rho_{\varepsilon(T_1)\varepsilon(T_2)}$ in the values of ε at two different periods of vibration (T_1 and T_2)

$$\rho_{\varepsilon(T_1)\varepsilon(T_2)} = \frac{\sigma_{\varepsilon(T_1)\varepsilon(T_2)}}{\sigma_{\varepsilon(T_1)} \cdot \sigma_{\varepsilon(T_2)}} \quad (10)$$

where $\sigma_{\varepsilon(T_1)\varepsilon(T_2)}$ is the covariance of $\varepsilon(T_1)$ $\varepsilon(T_2)$, $\sigma_{\varepsilon(T_1)}$ is the standard deviation of $\varepsilon(T_1)$ and $\sigma_{\varepsilon(T_2)}$ is the standard deviation of $\varepsilon(T_2)$. The single ground motion is artificially generated by means of the program SIMQKE, as a series of sinusoidal waves characterised by different amplitudes and phase angles. The significant duration of the ground motion $D_{SR}(5-95\%)$ between the moments corresponding to 95% and 5% of the total Arias intensity is forced to be equal to the mean value suggested by Bommer [[5]]. This value is only marginally variable with the return period of the earthquake and ranges from about 5 to 7 s. The accelerograms are enveloped by means of a compound intensity function that consists of three branches: the first branch is represented by a power function, the second is a constant function (strong motion phase) and the third is a function with exponential decay. As an example, the suites of the acceleration spectra corresponding to the obtained accelerograms (return period of 689 years) are reported in Figure 1b along with their median spectrum and the expected median spectrum.

SINGLE-DEGREE-OF-FREEDOM SYSTEMS

The fragility functions are first evaluated for SDOF systems consisting of a vertical rigid cantilever element with a rotational spring at the base and a mass m at the top. The SDOF systems have five different periods of vibration (0.2, 0.6, 1.2, 1.8 and 3.0 s) and four different moment-rotation models of the rotational spring. Specifically, the selected models of the rotational spring are elastic-perfectly plastic (later named model #1), elastic with hardening (model #2), elastic-plastic with degradation of stiffness and strength (model #3) and elastic-plastic with degradation of stiffness and strength and pinching (model #4). Further, four values (0, 0.0025, 0.05 and 0.1) are considered for the interstorey drift sensitivity coefficient θ_{el} given by the following relationship

$$\theta_{el} = \frac{Pu}{Vh} \quad (11)$$

where P is the vertical force at the top of the SDOF system, V is a horizontal force at the top of the system, u is the elastic horizontal top displacement caused by V and h is the height of the system. Given the period of vibration of the SDOF system and the mass m , the lateral stiffness K is obtained as $K=m(2\pi/T)^2$. The yielding shear force f_y of the SDOF system is obtained dividing the force $f_0 = mS_a^{475}(T_1)$ corresponding to the elastic pseudo-acceleration by a behaviour factor q equal to 6. Hence, the rotational stiffness $k_\phi = K \cdot h^2$ and the yielding bending moment M_y of the rotational spring at the base is $M_y = f_y \cdot h$.

The rotational stiffness of the spring of models #1 and #2 is equal to k_ϕ whereas the yielding bending moment is equal to M_y . The kinematic hardening ratio of model #2 is equal to 0.03. The backbone of model #3 (modified Ibarra-Medina-Krawinkler deterioration model with peak oriented hysteretic response [[10]]) is characterised by six parameters, namely the initial elastic stiffness k_ϕ , the yielding bending moment M_y , the hardening ratio of the post-yielding branch α_s (equal to 0.03), the ratio ϕ_c/ϕ_y of the rotation corresponding to the maximum bending moment to the rotation corresponding to the yield bending moment (equal to 6), the ratio M_r/M_y of the residual bending moment to the yielding bending moment (equal to 0.2) and the ratio α_c of the slope of the softening branch to the slope of initial elastic response (equal to 0.10). The degradation of the mechanical properties is ruled by the parameters γ_s , γ_c , γ_k , γ_a and c that model the basic strength deterioration (γ_s), the post-capping strength deterioration (γ_c), the unloading stiffness deterioration (γ_k), the accelerated reloading stiffness deterioration (γ_a) and the rate of deterioration (c) of the evaluated hysteretic parameter (strength or stiffness). The values of the parameters γ_s , γ_c , γ_k , γ_a and c are fixed here based on the results of experimental tests carried out by other researchers [[10]]. In particular, two combinations of the parameters γ_s , γ_c , γ_k , γ_a are considered. The first combination is distinctive of members with low degradation (e.g. steel members) and is defined by values of γ_s , γ_c , $\gamma_a=100$ and $\gamma_k=200$, whereas the second combination is characteristic of members with rapid degradation (wood or reinforced concrete members) and is defined by values of γ_s , γ_c , $\gamma_a=25$ and $\gamma_k=50$. In all the analysed cases, the parameter c is fixed equal to 1 [[11]]. Model #4 is similar to model #3 except for pinching. The values of parameters κ_d and κ_r responsible for pinching are equal to 0.25. Most of the considered models are plotted in Figure 2 subjected to the loading protocol proposed by the Consortium of Universities for Research in Earthquake Engineering (CUREE) [[12]].

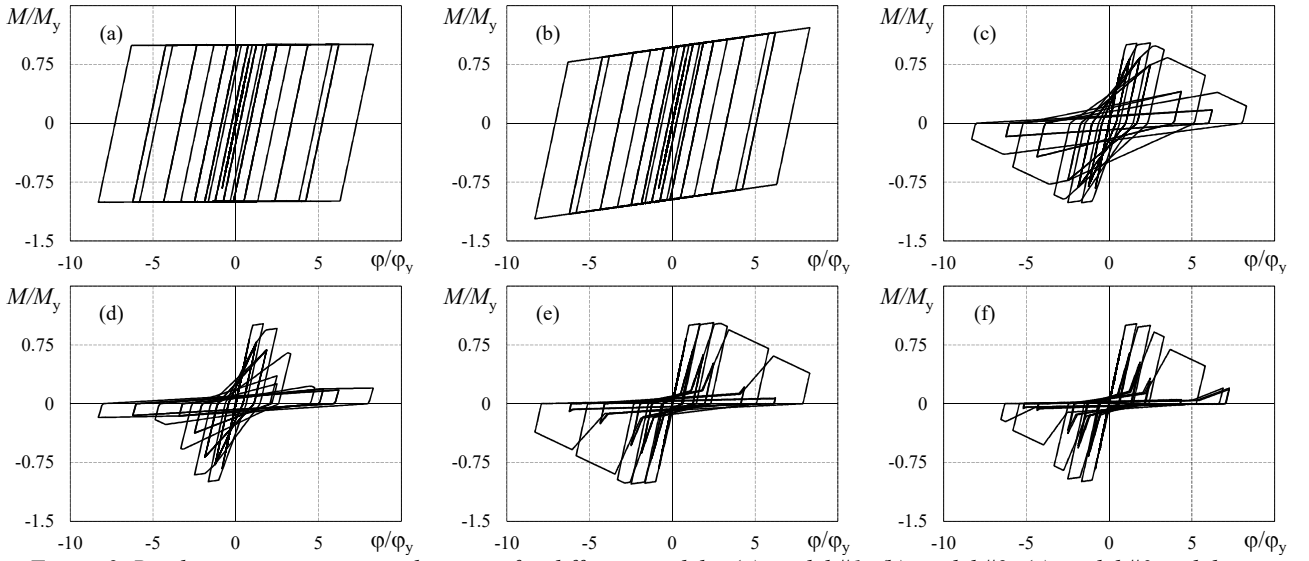


Figure 2. Bending moment-rotation diagrams for different models: (a) model #1, (b) model #2, (c) model #3 with low degradation, (d) model #3 with rapid degradation, (e) model #4 with low degradation, (f) model #4 with rapid degradation.

NUMERICAL ANALYSES OF SDOF SYSTEMS

The response of the SDOF system is evaluated in terms of the maximum displacement ductility demand and the limit state is assumed achieved if the maximum displacement ductility demand is higher than a specified limit value. This latter ductility demand is equal to 1/2, 1 or 4/3 times the maximum ductility demand μ_d accepted under earthquakes with return period equal to 475 years. The proportions of the three limit ductility demands aim to replicate those reported in Eurocode 8 for the verification of the damage limitation, significant damage and near collapse limit states of ductile members. The limit ductility demand μ_d is assumed equal to the behaviour factor considered in design and thus equal to 6.

To evaluate the impact of the variation of the elastic response spectrum shape with the selected IM, the multistripe analysis is first carried out with accelerograms characterised by median response spectrum shape variable with IM (later named analysis #1) and then with accelerograms characterised by median response spectrum shape invariable with IM (analysis #2). The generic suite of accelerograms used in analysis #2 is obtained by scaling the suite used in analysis #1 with regards to a return period of 475 years so that the median spectral acceleration of the scaled suite at the period of vibration of the SDOF system equals that prescribed by INGV for the considered period of vibration and earthquake return period. In any case, parameters θ and β of the fragility curves of the SDOF systems are calculated by means of Eq. (4) and then the mean annual frequency of exceedance of the limit state function is calculated based on the fragility curves and the mean seismic hazard $\bar{\lambda}_s(s)$ of the site. The difference between the responses of the two analyses is synthetically represented by means of the parameter

$$Er_{1-2}(\%) = (\lambda_{LS,1} - \lambda_{LS,2}) / \lambda_{LS,2} \cdot 100 \quad (12)$$

where $\lambda_{LS,1}$ and $\lambda_{LS,2}$ are the mean annual frequencies of exceedance of the assigned limit state function by means of analyses #1 and #2, respectively. A third analysis (analysis #3) is also carried out to evaluate the influence of the scattering of the spectral responses about their mean value. In this case, the mean annual frequency of exceedance ($\lambda_{LS,3}$) is obtained from accelerograms characterised by virtually null standard deviation and response spectrum shape and ground motion duration invariable with the magnitude of the earthquake. As in analysis #2, the median response spectrum shape and the ground motion duration used in analysis #3 are those corresponding to a return period of 475 years in analysis #1. In particular, the generic median response spectrum used in analysis #3 is obtained by scaling that used with regards to a return period of 475 years so that the median spectral acceleration of the scaled suite at the period of vibration of the SDOF system equals that prescribed by INGV for the considered period of vibration and earthquake return period. The mean annual frequency of exceedance resulting from analysis #3 ($\lambda_{LS,3}$) is compared to $\lambda_{LS,2}$ and the percentage difference is evaluated by means of the parameter

$$Er_{3-2}(\%) = (\lambda_{LS,3} - \lambda_{LS,2}) / \lambda_{LS,2} \cdot 100 \quad (13)$$

The values of Er_{1-2} are plotted in Figure 3 as a function of the period of vibration of the SDOF system for some models of therotational spring and for ductility demands equal to 1/2, 1 or 4/3 times the maximum ductility demand μ_d . The four lines

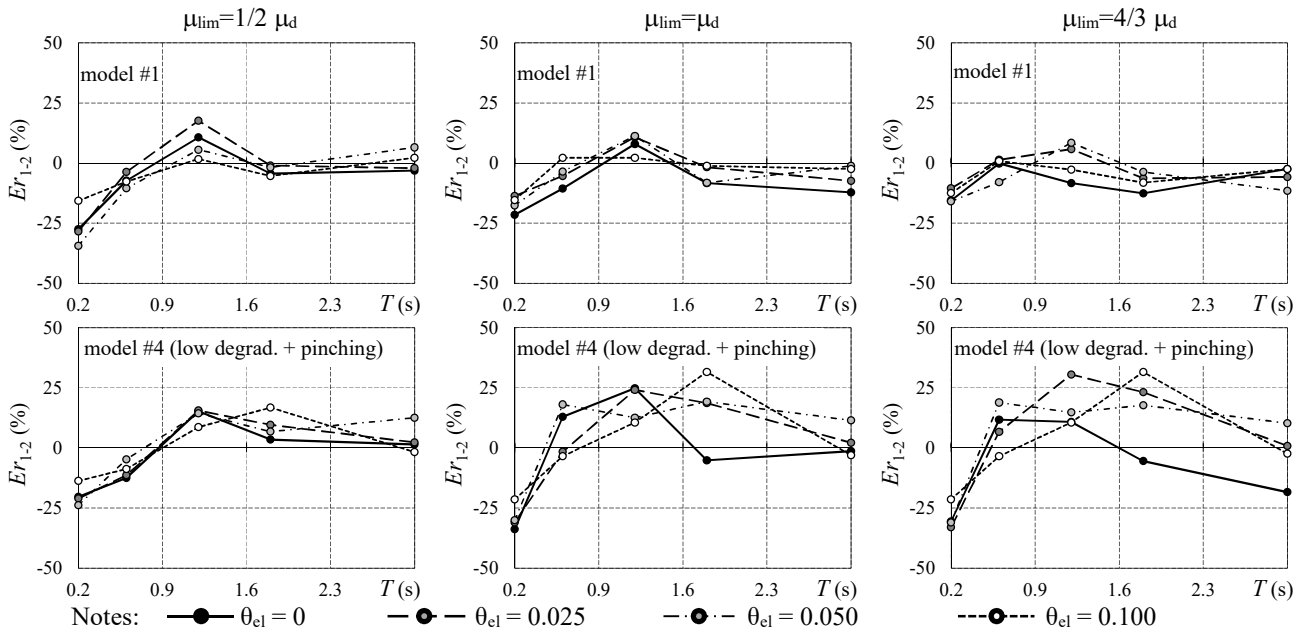


Figure 3. Parameter Er_{1-2} for SDOF systems characterized by model #1, peak-oriented model (model #4) with low degradation and pinching.

reported on each coordinate plane represent the response of systems characterized by different values of the interstorey drift sensitivity coefficient. The numerical analyses show that the percentage error Er_{1-2} corresponding to the period $T=0.20$ s is virtually always negative and often higher (in absolute) than that relative to higher periods of vibration. The maximum negative error (in absolute) is equal to 30% and found for the peak-oriented model (model #4) with low degradation and pinching. Only slightly lower negative errors (20-25% in absolute) are found for most of the other models considered. Positive values of Er_{1-2} are instead generally found for periods of vibration higher than about 0.50-0.60 s. They are often lower than 10 % and significant (about 30%) only in the case of use of the peak-oriented model (model #4). For SDOF systems characterised by model #1, the parameter Er_{1-2} does not show significant variations with the interstorey drift sensitivity coefficient θ_{el} . This trend is independent of the period of vibration of the system and model of the rotational spring at the base of the SDOF system.

To explain the obtained sign of the percentage errors, the adopted procedure is described for some of the considered systems. Specifically, attention is focused on the SDOF systems with period of vibration $T=0.20$ s or 1.20 s and model #4 with low degradation and pinching. Figure 4 shows the median spectrum of the accelerograms used for analysis #1 for $T_R=50$ years (Fig. 4a) and $T_R=2500$ years (Fig. 4b) along with the median spectra of the accelerograms used in analysis #2 for systems with $T=0.20$ s or 1.20 s. In the case of $T_R=50$ years (low IMs), when the accelerograms are scaled to match the target spectrum at $T=0.20$ s (i.e. in analysis #2), the obtained spectral accelerations are significantly larger than those of analysis #1 for $T>0.20$ s. An opposite trend is recorded for high intensity measures (Fig. 4b). Instead, when the accelerograms are scaled to analyze the system with $T=1.20$ s, the spectral accelerations corresponding to $T>1.20$ s are slightly larger than those of the target spectrum. It is worth noting that the spectral accelerations corresponding to periods larger than those of the considered systems affect the response because yielding of the rotational spring at the base of the system causes an increase in the period of vibration. Consequently, for short period systems, the probability of exceedance of the assigned limit state function at low IM by means of analysis #2 ($p_{LS,2}$) is expected to be larger than that by means of analysis #1 ($p_{LS,1}$). An opposite trend is expected for long period systems. Figure 5a and b shows the fragility functions corresponding to ductility demands equal to the maximum ductility demand μ_d obtained from analyses #1 and #2 for the systems described above. If the equal displacement rule was rigorously valid, the number of exceedances of the maximum ductility demand μ_d for an intensity measure equal to $S_a^{475}(T_i)$ should be equal to 50% of the total number of ground motions. This applies to the response obtained by both analyses #1 and #2 because the ground motions used in the two analyses at this intensity measure are the same. Hence, the fragility curves obtained from analyses #1 and #2 should meet at a point characterised by an IM = $S_a^{475}(T_i)$ and probability of exceedance = 50%. Instead, especially for short period systems, the displacement developed by nonlinear dynamic analysis is generally larger than that predicted by the equal displacement rule. As an example, the number of exceedances recorded at an IM = $S_a^{475}(T_i)$ in the SDOF with $T=0.20$ s is close to 100% and the slope of the fragility function is governed by the response for IMs lower than $S_a^{475}(T_i)$. Similarly, in the system with $T=1.20$ s the number of exceedances at an IM = $S_a^{475}(T_i)$ is 70%. Based on the considerations on the shape of the spectra and on the approximation of the equal displacement rule, the fragility curve obtained by analysis #2

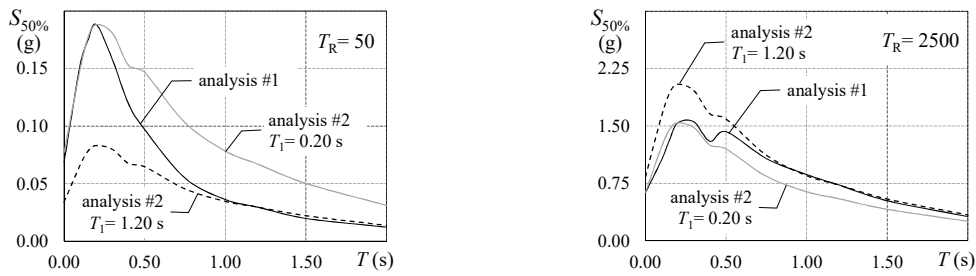


Figure 4. Target median spectrum and scaled median spectra for SDOF systems with $T=0.20$ s and $T=1.20$ s.

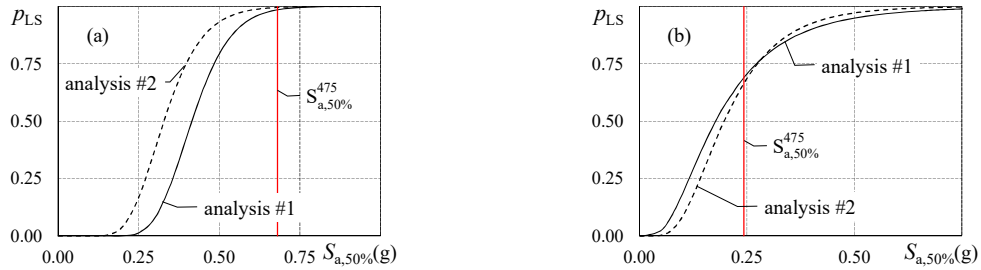


Figure 5. Fragility functions of analyses #1 and #2 for model #4, $\mu_{lim}=\mu_d$, $\theta_{el}=0$ and (a) $T=0.20$ s (b) $T=1.20$ s.

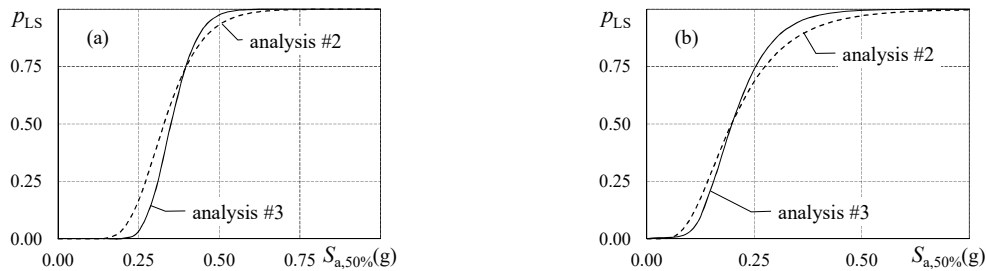


Figure 6. Fragility functions of analyses #2 and #3 for model #4, $\mu_{lim}=\mu_d$, $\theta_{el}=0$ and (a) $T=0.20$ s, (b) $T=1.20$ s.

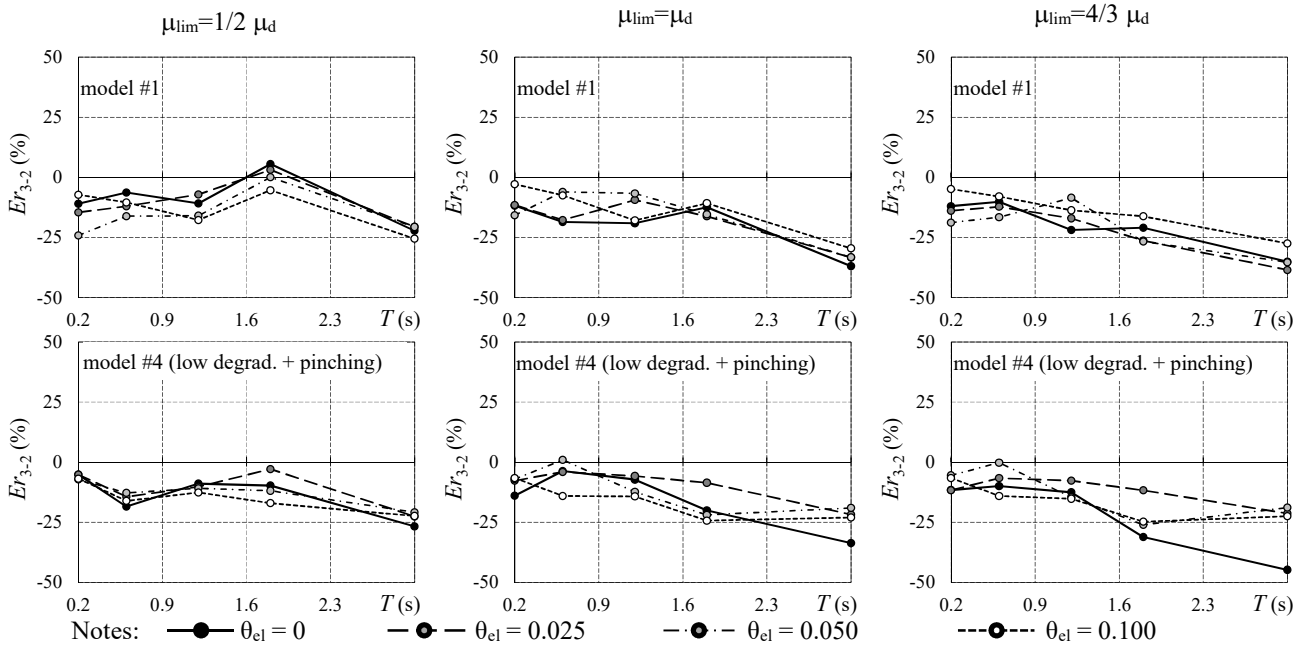


Figure 7. Parameter Er_{3-2} for SDOF systems characterized by model #1 and peak-oriented model (model #4) with low degradation and pinching.

for the SDOF with $T=0.20$ s is on the left of that obtained by analysis #1 (Figure 5a) and the percentage error Er_{1-2} is always negative. In the case of $T=1.20$ s, $p_{LS,1}$ is higher than $p_{LS,2}$ for IMs lower than those corresponding to $T_R=475$ and lower for the other IMs. These trends in the probability of exceedance of the assigned limit state function combine with the shape of the usual seismic hazard curves to lead to the results in Figure 3. In fact, the contribution of the upper part of the fragility curve to the mean annual frequency of exceedance is generally lower than that of the lower part because of the lower ordinates of the seismic hazard curve at high IMs (see Eq. 7).

Processing of data from analyses #2 and #3 highlights results that may be partly explained by recalling that in analysis #3 the spectral accelerations are characterised by a virtually null dispersion about their mean value. In fact, as shown in Figure 6 for some systems characterised by elastic-perfectly plastic model and periods of vibration equal to either 0.2 or 1.2 s, if the suite of accelerograms is scaled to low IMs the probability of exceedance $p_{LS,3}$ is likely to be lower than that ($p_{LS,2}$) resulting from analysis #2 (in which the dispersion of the spectral accelerations is significant but the shape of the median acceleration spectrum is constant with IM). Conversely, if the suite of accelerograms is scaled to high IMs the probability of exceedance $p_{LS,3}$ is likely to be higher than $p_{LS,2}$. Again, these trends are amplified by the usual shape of the seismic hazard curve to calculate the mean annual frequency of exceedance. Owing to this, errors Er_{3-2} are generally negative and increase in absolute with the period of vibration of the system to reach values that may be as high as 30% (Fig. 7).

CONCLUSIONS

The numerical analyses lead to the following main conclusions:

- the variation of the shape of the response spectrum with the earthquake return period may be important for an accurate evaluation of the mean annual frequency of exceedance of assigned limit states. The errors linked to the use of invariable spectral shapes appear to be significant for structures with fundamental period of vibration similar to the one corresponding to the main variation in the normalized response spectrum. These errors also appear to be increasing with the ductility demand and with the degradation of the cyclic inelastic response.
- the use of accelerograms characterized by a virtually null scattering of the spectral accelerations about the mean value always leads to significant underestimation of the mean annual frequency of exceedance of a given limit state.

The authors note that the analyses reported here have been carried out for a single specific site of the Italian territory. This site has not been selected to magnify the relevance of the addressed problem but only to be characterised by a medium peak ground acceleration for an earthquake return period of 475 years. Even if not proved, this may presage that the extent of the problem could be elsewhere even larger than already highlighted in this paper.

REFERENCES

- [1] Jalayer, F., and Cornell, C.A. (2009) Alternative non-linear demand estimation methods for probability-based seismic assessments. *Earthquake Engineering & Structural Dynamics*; 38: 951-972.
- [2] DM 14 January 2008, published on Gazzetta Ufficiale n. 29, 4 febbraio 2008 - Suppl. Ordinario n. 30.
- [3] Calvi, G.M., Rodrigues, D., and Silva, V. (2018) Introducing new design spectra derived from Italian recorded ground motions 1972 to 2017. *Earthquake Engineering & Structural Dynamics*; 47(13): 2644-2660.
- [4] Meletti, C., and Montaldo, V. (2007) Stime di pericolosità sismica per diverse probabilità di superamento in 50 anni: valori di a_g . Progetto DPC-INGV S1, Deliverable D2; <http://esse1.mi.ingv.it/d2.html>.
- [5] Bommer, J.J., Stafford, P.J., and Alarcón, J.E. (2009) Empirical Equations for the Prediction of the Significant, Bracketed, and Uniform Duration of Earthquake Ground Motion. *Bulletin of the Seismological Society of America*; 99 (6): 3217-3233.
- [6] Zentner, I. (2014) A procedure for simulating synthetic accelerograms compatible with correlated and conditional probabilistic response spectra. *Soil Dynamics and Earthquake Engineering*; 63: 226-233.
- [7] Baker, J.W. (2015) Efficient analytical fragility functions fitting using dynamic structural analysis *Earthquake Spectra*; 31(1): 579-599.
- [8] CNR-DT 212/2013, *Istruzioni per la Valutazione Affidabilistica di Edifici Esistenti*, Consiglio Nazionale delle Ricerche, Roma, 14 maggio 2014.
- [9] Cimellaro, G.P. (2013) Correlation in spectral acceleration for earthquakes in Europe. *Earthquake Engineering & Structural Dynamics*; 42: 623-633.
- [10] Ibarra, L., Medina, R., and Krawinkler, H. (2005) Hysteretic models that incorporate strength and stiffness deterioration. *Earthquake Engineering & Structural Dynamics*; 34: 1489-1511.
- [11] Rahnema, M., and Krawinkler, H. (1993) Effect of soft soils and hysteresis models on seismic design spectra. John A. Blume Earthquake Engineering Research Center Department of Civil Engineering, Stanford University; Report No. 108.
- [12] Krawinkler, H., Parisi, F., Ibarra, L., Ayoub, A., and Medina, R. (2000) Development of a testing protocol for woodframe structures. CUREE Publication No. W-02.